Cell. Mol. Life Sci. (2016) 73:649–666
DOI 10.1007/s00018-015-2018-8

Cellular and Molecular Life Sciences

ORIGINAL ARTICLE

Shear stress mediates exocytosis of functional TRPV4 channels in endothelial cells

Sara Baratchi[1] · Juhura G. Almazi[1] · William Darby[1] · Francisco J. Tovar-Lopez[2] · Arnan Mitchell[2] · Peter McIntyre[1]

Received: 9 March 2015 / Revised: 25 July 2015 / Accepted: 6 August 2015 / Published online: 20 August 2015

Abstract Mechanosensitive ion channels are implicated in the biology of touch, pain, hearing and vascular reactivity; however, the identity of these ion channels and the molecular basis of their activation is poorly understood. We previously found that transient receptor potential vanilloid 4 (TRPV4) is a receptor operated ion channel that is sensitised and activated by mechanical stress. Here, we investigated the effects of mechanical stimulation on TRPV4 localisation and activation in native and recombinant TRPV4-expressing cells. We used a combination of total internal reflection fluorescence microscopy, cell surface biotinylation assay and Ca^{2+} imaging with laser scanning confocal microscope to show that TRPV4 is expressed in primary vascular endothelial cells and that shear stress sensitises the response of TRPV4 to its agonist, GSK1016790A. The sensitisation was attributed to the recruitment of intracellular pools of TRPV4 to the plasma membrane, through the clathrin and dynamin-mediated exocytosis. The translocation was dependent on ILK/Akt signalling pathway, release of Ca^{2+} from intracellular stores and we demonstrated that shear stress stimulated phosphorylation of TRPV4 at tyrosine Y110. Our findings implicate calcium-sensitive TRPV4 translocation in the regulation of endothelial responses to mechanical stimulation.

Keywords TRPV4 · Endothelium · Shear stress · Translocation · Ca^{2+} · Mechanotransduction

Introduction

Transduction of mechanical forces into intracellular biochemical signals (mechanosensation), is crucial for many of our senses including touch, hearing and balance [1]. It is also necessary in embryonic development [2, 3] and adult physiology, and is important in different conditions and diseases including pain, atherosclerosis [4], hypertension [5], cancer [6] and muscular dystrophy [7].

Blood flow exerts friction (or shear stress) on the vascular endothelium and pressure on the vessel walls. These forces produce myogenic tone that controls the diameter of the vessels [5, 8]. Endothelial dysfunction results in abnormal regulation of vessel diameter and hence blood flow, and is a major risk factor for cardiovascular diseases [5].

Mechanotransduction is a dynamic response that is mediated by relative movement of different subcellular structures which result in opening of ion pores and depolarisation of the cell [1]. In bacteria, this is mediated by directly activated mechanosensitive ion channels in the outer membrane [9]. However, in multicellular organisms depolarisation involves more complex transduction mechanisms, such as signalling from mechanoreceptors such integrins, cytoskeletal components and ion channels [10]. Recent studies have highlighted the role ion channels in physiology of mechanotransduction including channels from the transient receptor potential (TRP) family,

Electronic supplementary material The online version of this article (doi:10.1007/s00018-015-2018-8) contains supplementary material, which is available to authorized users.

✉ Peter McIntyre
peter.mcintyre@rmit.edu.au

[1] School of Medical Sciences and Health Innovations Research Institute, RMIT University, Melbourne, VIC 3083, Australia

[2] School of Electrical and Computer Engineering, RMIT University, Melbourne, VIC 3001, Australia

mechano-gated K^+ channels, amiloride-sensitive Na^+ channel or recently discovered Piezo ion channels [9, 11].

Recent studies have demonstrated that mechanotransducers are often dynamic and can undergo assembly, disassembly and movement [12–14] and these processes control the transduction of mechanical forces [15].

Although little is known of how mechanotransduction is initiated in endothelium, it has been shown that intracellular Ca^{2+} ($[Ca^{2+}]_i$) controls the vasoregulatory pathways initiated by vascular endothelial cells, and is also important in controlling vascular tone and homeostasis by activating endothelial nitric oxide synthase and calcium-activated potassium channels [16]. The two most important mechanisms for regulation of $[Ca^{2+}]_i$ are release of Ca^{2+} from intracellular stores and influx of extracellular Ca^{2+} via calcium permeable channels [17]. The TRP vanilloid 4 (TRPV4) channel, is a non-selective cation channel from the TRP super family that has moderately high calcium permeability [17, 18]. TRPV4 is expressed widely in epithelia and vascular endothelium. Several reports have suggested that TRPV4 mediated Ca^{2+} entry plays a key role in shear stress-induced vasodilation [19, 20]. We have shown that shear stress increases $[Ca^{2+}]_i$ in aortic endothelial cells via calcium influx through TRPV4. Moreover, removal of extracellular calcium or application of a specific TRPV4 antagonist to endothelial cells, abolishes the shear stress effect on $[Ca^{2+}]_i$ [21]. These observations suggest Ca^{2+} entry through TRPV4 directly or indirectly controls mechanosensitivity of endothelial cells [21].

Despite the known role of TRPV4 in critical endothelium-dependent vasoregulatory pathways, the molecular basis of TRPV4 mechanosensation is not well understood. The activity of ion channels is regulated in a variety of ways that can include alteration in gene expression and intracellular trafficking [22, 23] and post-translational modifications such as phosphorylation. Phosphorylation of TRPV4 at tyrosine 110 is necessary for its response to shear stress and hypotonic stimulation [24], while *N*-linked glycosylation at asparagine 561 regulates the TRPV4 response to hypotonicity [25]. Cell surface expression of TRPV4 depends on many factors, including protein synthesis and correct folding in the endoplasmic reticulum (ER), glycosylation [25], subunit assembly [26] as well as recycling and degradation [27]. The effects of changes in the ion channels trafficking and the formation of functional channels at the plasma membrane is of increasing interest [28].

In this study, we investigate the response of endothelial cells to shear stress in vitro. Using a combination of calcium imaging, total internal reflection fluorescent microscopy (TIRFM) and biochemical techniques, we show that shear stress increases $[Ca^{2+}]_i$ though TRPV4-dependent calcium influx, as well as Ca^{2+} release from intracellular sources. The TRPV4-dependent shear response involves exocytosis of the channel from recycling endosomes and requires an intact actin cytoskeleton. We also demonstrate that recruitment is dependent on PKA, the small GTPase Rac1 and ILK/Akt signalling.

Methods

Compounds and buffers

For all the imaging experiments, cells were immersed in standard Hanks' Balanced Salt Solution (HBSS) buffer containing: 140 mmol/L NaCl, 5 mmol/L KCl, 10 mmol/L HEPES, 11 mmol/L D-glucose, 1 mmol/L $MgCl_2$, 2 mmol/L $CaCl_2$, and 2 mmol/L probenecid, adjusted to pH = 7.4 [21]. For calcium-free buffer, $CaCl_2$ in HBSS buffer was replaced with 2 mmol/L EGTA (ethylene glycol tetraacetic acid).

GSK1016790A, TRPV4-selective agonist; ruthenium red, non-selective TRP antagonist; brefeldin A, inhibitor of intracellular protein transport; GSK690693, Akt inhibitor; Cytochalasin D, inhibitor of actin polymerisation were purchased from (Sigma-Aldrich, St. Louis, MO). HC067047, TRPV4-selective antagonist; (Santa Cruz Biotechnology, Santa Cruz, CA), Pipstop^{2M}, Clathrin inhibitor (Abcam), Cpd 22, Integrin-linked kinase (ILK) inhibitor (Calbiochem), NSC 23766, Rac1 inhibitor (Santa Cruz) were dissolved according to suppliers instruction and diluted in HBSS prior to experimentation and corresponding vehicles (0.1 % v/v dH_2O or 0.1 % v/v DMSO) were used as controls.

Cell culture, molecular biology and gene transfection

Human Umbilical Vein Endothelial Cells (HUVECs) were grown in EGM^{TM}-2 media supplemented with SingleQuots^{TM} kit (Lonza, Walkersville MD, USA). HEK293 T-Rex cell lines (Life Sciences) stably expressing TRPV4, TRPV4-Y110F and TRPV4-Y805F were generated as described [29, 30] and grown in (Dulbecco's Modified Eagle's medium) supplemented with 10 % foetal bovine serum, hygromycin (50 μg/ml), and blasticidin (5 μg/ml).

In vitro generation of shear stress and $[Ca^{2+}]_i$ measurement

Details of shear stress experiments are reported elsewhere [21]. Briefly, for each experiment, loaded cells were excited with a 488 nm laser using Nikon A1 laser scanning confocal microscope and fluorescence emission was

detected using a photomultiplier tube following a 525/50 nm band-pass filter and a PlanFluor 10× objective with a numerical aperture of 0.30. Calcium influx was measured as an increase in the fluorescent intensity of Fluo-4AM and normalised to the fluorescent intensity of resting cells.

Measurement of changes in $[Ca^{2+}]_i$ levels were performed from the entire endothelial cell. Regions of 300 μm × 200 μm were selected for each region of shear stress and all cells within that region have been analysed. The cell area was measured by drawing a region of interest drawn (ROIs) around single endothelial, automatically using NIS element viewer (Nikon Instruments Inc.). To quantify changes in $[Ca^{2+}]_i$, the average intensity of several ROIs has been measured and results are reported as ratio of F1/F0.

At the end of each experiment, the cells were stained with propidium iodide (PI) (10 μg/ml) and only experiments with more than 80 % viable cells were analysed. All imaging experiments were performed at 37 °C unless otherwise stated.

Data are shown as mean ± standard deviation of at least four independent experiments and 30–40 cells were analysed in each experiment. For statistical analysis, Student's *t* test or one-way ANOVA was performed using Prism 6 (GraphPad software) and $P < 0.05$ was considered to be significant.

Biotinylation of surface proteins

HEK293 and HUVECs were grown in μ-slide (Ibidi) to confluence, incubated with reagents or appropriate controls and subjected to shear stress of 10 dyn/cm^2 for 30 s. After stimulation, EZ-Link Sulfo-NHS-SS linked biotin (0.5 mg/ml) in PBS was added to the cells and incubated on ice for 30 min. Following stimulation the reaction was quenched with 50 mmol/L glycine and excess biotin removed with PBS. Lysates were prepared in standard lysis buffer (1 mmol/L EDTA, 1 mmol/L EGTA, 30 mmol/L NaCl, 50 mmol/L $Na_2H_2PO_4$, 2 mmol/L PMSF, Halt Protease Inhibitor Cocktail (Pierce) and 1 % Triton-X-100). Samples were normalised for the protein concentration and incubated with streptavidin beads over night at 4 °C. The samples were washed 3 times with lysis buffer and eluted by boiling in SDS denaturing sample buffer (62.5 mmol/L Tris–HCl (pH 6.8), 10 % glycerol, 2 % SDS, 0.1 % bromphenol blue, 50 mmol/L DTT, 0.5 mol/L-mercaptoethanol) and western immuno-blotted using standard protocols using rabbit anti-TRPV4 antibody (ab39260, Abcam, dilution 1/2500) and mouse anti-cadherin antibody (C1821, Sigma, dilution 1/2500). The bands were visualised using HRP conjugated anti-rabbit antibody (SC2389, Santa Cruz, dilution 1/5000) and HRP conjugated anti-mouse antibody (SC-2371, Santa Cruz, dilution 1/5000). The cadherin band density was used to normalise for surface protein concentration. Probing for GAPDH with anti-GAPDH antibody (Sigma-Aldrich, dilution 1/5000) did not show any staining, confirming the absence of labelled intracellular proteins.

Protein expression and purification using Strep-Tactin affinity chromatography

A C-terminal strep-tag II (Trp-Ser-His-Pro-Gln-Phe-Glu-Lys) tag was introduced using a QuickChange kit (Qiagen) in hTRPV4 pcDNA5/FRT/TO followed by transfection into TRex cells. TRPV4 expression was induced with 0.1 μg/ml tetracycline in DMEM for 16–20 h. Shear stress was applied to cells as described above.

The cells were lysed using the lysis buffer (50 mmol/L NaH_2PO_4, 300 mmol/L NaCl pH 8 with 1 % Triton X-100, 1 mmol/L EGTA, 1 mmol/L EDTA, 2 mmol/L PMSF, 1 % Halt Phosphatase Inhibitor Cocktail [(Thermo scientific), 1 % protease inhibitor cocktail (Sigma)]. DNA was sheared by passage through needle and syringe and debris removed by centrifugation (16,000×*g*, 5 min, 4 °C). Strep-Tactin Superflow Resin was added (50 μl per 1 ml of lysate) and mixed gently at 4 °C for 60 min. The beads were washed by centrifugation (1000×*g*), once with lysis buffer and again with wash buffer (50 mmol/L NaH_2PO_4 and 300 mmol/L NaCl) to remove detergents. The protein-bound beads were incubated in 1 % rapigest (Waters) in 50 mmol/L ammonium bicarbonate (ABC) for 30 min, followed by reduction with 5 mmol/L DTT and alkylation with 15 mmol/L iodoacetamide. The samples were further digested with 0.1 % rapigest and 3 % trypsin in ABC for 16 h at 37 °C and the peptides acidified with 5 % trifluoroacetic acid and incubated at 37 °C for 1 h prior to concentration and desalting on a C18 micro-column.

Selective reaction monitoring assay

Signature proteotypic peptides were predicted from protein sequences from the NCBI database using the Skyline software 2.0 (MacCoss Lab, University of Washington). Tryptic peptides with phosphosite residues of interest were selected and both the phosphorylated and unmodified peptides monitored. For each peptide, 3 selected reaction monitoring (SRM) transitions were selected, with a precursor charge of +2 and a y-fragment charge of +1 (Table 1). Collision energy was then optimised using Skyline software. Peptide retention times were determined in pilot experiments and the best transitions were selected for analysis.

Table 1 Transitions used for the SRM assay of sp|Q9HBA0|TRPV4_HUMAN

	Precursor (*m*/*z*)	Fragment (*m*/*z*)	Peptide	Y ions	Label
Y110	808.3286	1114.461	APMDSLFDpYGTYR	y8	–
	808.3286	1001.376	APMDSLFDpYGTYR	y7	–
	808.3286	854.308	APMDSLFDpYGTYR	y6	–
	813.3327	1124.469	APMDSLFDpYGTYR	y8	13C/15N
	813.3327	1011.385	APMDSLFDpYGTYR	y7	13C/15N
	813.3327	864.3163	APMDSLFDpYGTYR	y6	13C/15N
	768.3454	1034.494	APMDSLFDYGTYR	y8	–
	768.3454	921.4101	APMDSLFDYGTYR	y7	–
	768.3454	774.3417	APMDSLFDYGTYR	y6	–
	773.3495	1044.502	APMDSLFDYGTYR	y8	13C/15N
	773.3495	931.4184	APMDSLFDYGTYR	y7	13C/15N
	773.3495	784.35	APMDSLFDYGTYR	y6	13C/15N
Y805	951.3964	1314.623	NETpYQYYGFSHTVGR	y11	–
	951.3964	1186.564	NETpYQYYGFSHTVGR	y10	–
	951.3964	1023.501	NETpYQYYGFSHTVGR	y9	–
	956.4005	1324.631	NETpYQYYGFSHTVGR	y11	13C/15N
	956.4005	1196.572	NETpYQYYGFSHTVGR	y10	13C/15N
	956.4005	1033.509	NETpYQYYGFSHTVGR	y9	13C/15N
	911.4132	1314.623	NETYQYYGFSHTVGR	y11	–
	911.4132	1186.564	NETYQYYGFSHTVGR	y10	–
	911.4132	1023.501	NETYQYYGFSHTVGR	y9	–
	916.4173	1324.631	NETYQYYGFSHTVGR	y11	13C/15N
	916.4173	1196.572	NETYQYYGFSHTVGR	y10	13C/15N
	916.4173	1033.509	NETYQYYGFSHTVGR	y9	13C/15N
S162	939.4741	1138.698	GpSTADLDGLLPFLLTHK	y10	–
	939.4741	1081.677	GpSTADLDGLLPFLLTHK	y9	–
	939.4741	855.508	GpSTADLDGLLPFLLTHK	y7	–
	943.4812	1146.712	GpSTADLDGLLPFLLTHK	y10	13C/15N
	943.4812	1089.691	GpSTADLDGLLPFLLTHK	y9	13C/15N
	943.4812	863.522	GpSTADLDGLLPFLLTHK	y7	13C/15N
	899.4909	1138.698	GSTADLDGLLPFLLTHK	y10	–
	899.4909	1081.677	GSTADLDGLLPFLLTHK	y9	–
	899.4909	855.508	GSTADLDGLLPFLLTHK	y7	–
	903.498	1146.712	GSTADLDGLLPFLLTHK	y10	13C/15N
	903.498	1089.691	GSTADLDGLLPFLLTHK	y9	13C/15N
	903.498	863.522	GSTADLDGLLPFLLTHK	y7	13C/15N
S824	591.2768	1066.519	DRWpSSVVPR	y8	–
	591.2768	910.418	DRWpSSVVPR	y7	–
	591.2768	724.3389	DRWpSSVVPR	y6	–
	596.2809	1076.528	DRWpSSVVPR	y8	13C/15N
	596.2809	920.4265	DRWpSSVVPR	y7	13C/15N
	596.2809	734.3472	DRWpSSVVPR	y6	13C/15N
	551.2936	830.4519	DRWSSVVPR	y8	–
	551.2936	644.3726	DRWSSVVPR	y7	–
	551.2936	557.3406	DRWSSVVPR	y6	–
	556.2978	840.4602	DRWSSVVPR	y8	13C/15N
	556.2978	654.3809	DRWSSVVPR	y7	13C/15N
	556.2978	567.3488	DRWSSVVPR	y6	13C/15N

SRM analysis was performed using 4–6 biological replicates for each condition. Tryptic peptides were spiked with 5–10 fmol of 13C- and 15N-labelled synthetic peptides (JPT Peptide Technologies, Berlin, Germany). Peptides were purified using a C18 column prior to analysis using a TSQ Vantage triple quadrupole mass spectrometer (Thermo Scientific). Peptides were purified on a nanoUPLC Ultimate 3000 system (Thermo Scientific) coupled to a 150-mm fused silica column (75 μm inner diameter), packed with Acclaim PepMap RSLC resin (2 μm, 100Å, NanoViper (Thermo Scientific).

2 μl of peptide digests (10 μl) spiked with and 5–10 fmol of heavy labelled synthetic peptides were loaded on the column from a cooled (4 °C) autosampler. The separations were performed with a linear gradient from 2 to 45 % acetonitrile in 44 min (60 min method, Buffer A: 0.1 % formic acid in water, Buffer B: 0.1 % formic acid in acetonitrile) at a flow rate of 300 nl/min. The mass spectrometer was run in scheduled SRM mode (SRM detection time window, 300 s; target scan time, 1.5 s). Blank runs were performed between samples to avoid and assess sample carry-over. SRM acquisition was performed with Q1 and Q3 operated at unit resolution with a maximum 100 transitions per run.

Immunofluorescence

Cells were fixed with 4 % paraformaldehyde and permeabilised with 0.2 % Triton X-100 in PBS. Nonspecific binding was blocked with 2 % goat serum or 5 % BSA in PBS and probed with Atto 565-phalloidin (94072, Sigma-Aldrich, dilution 1/500) or anti-TRPV4 antibody (ab39260, Abcam, dilution: 1/200) and Alexa 488 anti-rabbit antibody (A11008, Invitrogen, dilution 1/400).

Evanescence field microscopy and image analysis

Live imaging experiments were performed at 27 °C. For the experiments in HEK293, cells were seeded inside the glass-bottomed microfluidic channel and transiently transfected with TRPV4-YFP (a kind gift from Dr. Shireen Lamande, Melbourne University, Australia) for 24 h. Before each experiment growth media was replaced with HBSS containing: 140 mM NaCl, 5 mM KCl, 10 mM HEPES, 11 mM D-glucose, 1 mM $MgCl_2$, 2 mM $CaCl_2$, 2 mM probenecid; pH 7.4. TRPV4 channel dynamics was visualised using Nikon Eclipse Ti inverted fluorescence microscope equipped with Apo TIRF 100× Oil/NA 1.49 objective under the control of NIS Element software. Coherent diode lasers at 488 nm were used for TIRF illumination and a Xenon arc lamp (Newport) filtered at 490 nm was used for reflection imaging. For real-time experiments, images were acquired every 0.5 s for an overall time course of 1 min and then every minute for an overall time course of 5 min. Cells were imaged for 1 min before applying a shear stress of 10 dyn/cm^2 to establish a baseline. For live cell experiments, changes in EFF was determined by subtracting the projection of minimum intensity (EFFmin) of the whole movie from each image [EFF(t)] and normalising it to the background intensity measured in a region of interest outside the cell (EFFbck) with the following equation:

$$\Delta\mathrm{EFF} = \left(\frac{\mathrm{EFF}(t) - \mathrm{EFFmin}}{\mathrm{EFFmin} - \mathrm{EFFbck}}\right) \times 100.$$

Intracellular calcium assay and confocal microscopy

HUVECs were seeded at 2500 cells per well onto poly-L-lysine (100 μg/ml) coated 384-well plates, and cultured for 72 h. Prior to measurements the cells were washed with HBSS buffer at 37 °C prior to loading with Fura2-AM ester (2.5 μM) and pluronic acid (0.5 μM) for 30 min at 37 °C and 5 % CO_2 in the dark, followed by two washes with HBSS buffer.

Fluorescence was measured from the entire well at 340 and 380 nm excitation and 520 nm emission wavelengths using a FlexStation 3 plate reader (Molecular Devices, Synnyvale, CA) as described previously [21]. Fluorescence was recorded every 5.8 s and drug additions were made after 17 s to allow for baseline reading. Results are expressed as the 340/380 nm fluorescence ratio, proportional to intracellular calcium ($[Ca^{2+}]_i$) levels. Suitable concentrations of agonists and antagonists were obtained from the available literature or from concentration response curves.

For line scan analysis, confocal 3D reconstruction microscopy was used. Briefly, z-stacks with a spacing of 200 nm were acquired with a frame rate of 0.33 Hz, from bottom to the top of cells at 488 nm for YFP, and at 560 nm for Atto 565 by sequential scanning using 60×/NA 1.2 objective on the Nikon A1 confocal microscope. For each condition, at least 20 stacks were generated within 20 min. Deconvolution, and colocalisation analysis of YFP (for TRPV4) and Atto 565 (for actin) was performed using NIS element AR module as reported previously by others [31]. For colocalisation analysis, the Pearson's correlation value was generated using NIS elements AR module, which was proportional to the degree of colocalised pixels in the both fluorescent channels. The translocation and colocalisation of TRPV4 and actin were assessed on median slice of a confocal stack acquired for each image.

Statistics

Statistical analysis was performed using Student's *t* test or ANOVA with Graph pad prism software. Results are given as mean ± SEM and *P* value of less than 0.05 were considered significant (* $P < 0.05$, ** $P < 0.01$, *** $P < 0.001$).

Results

Shear stress sensitises agonist activation of TRPV4

TRPV4-expressing cells respond to shear stress by initiating TRPV4-mediated calcium influx [29]. We previously demonstrated in endothelial cells that, in the presence of the TRPV4-specific agonist GSK1016790A, shear stress sensitises increased intracellular $[Ca^{2+}]_i$ [21]. However, the mechanism mediating this response is not understood. To investigate the underlying process, we used the TRPV4 response to GSK1016790A as a sensitive and reliable measure of TRPV4 sensitisation in response to shear stress. Initially, HUVECs were exposed to physiologically relevant levels of shear stress, ranging from 0.6 to 10 dyn/cm^2, in presence of graded concentrations of GSK1016790A (0.1–20 nM). Changes in $[Ca^{2+}]_i$ were determined by confocal microscopy. At 0.1 nM GSK1016790A, shear stress caused only a weak response $[Ca^{2+}]_i$ response (Fig. 1a). However, at concentrations between 1 and 10 nM, increasing shear stress from 1 to 10 dyn/cm^2 resulted in significant sensitisation of TRPV4 response to the agonist (Fig. 1b–f) ($P < 0.01$). Sensitisation was not significant at 20 nM GSK1016790A, most likely because the channel was maximally activated.

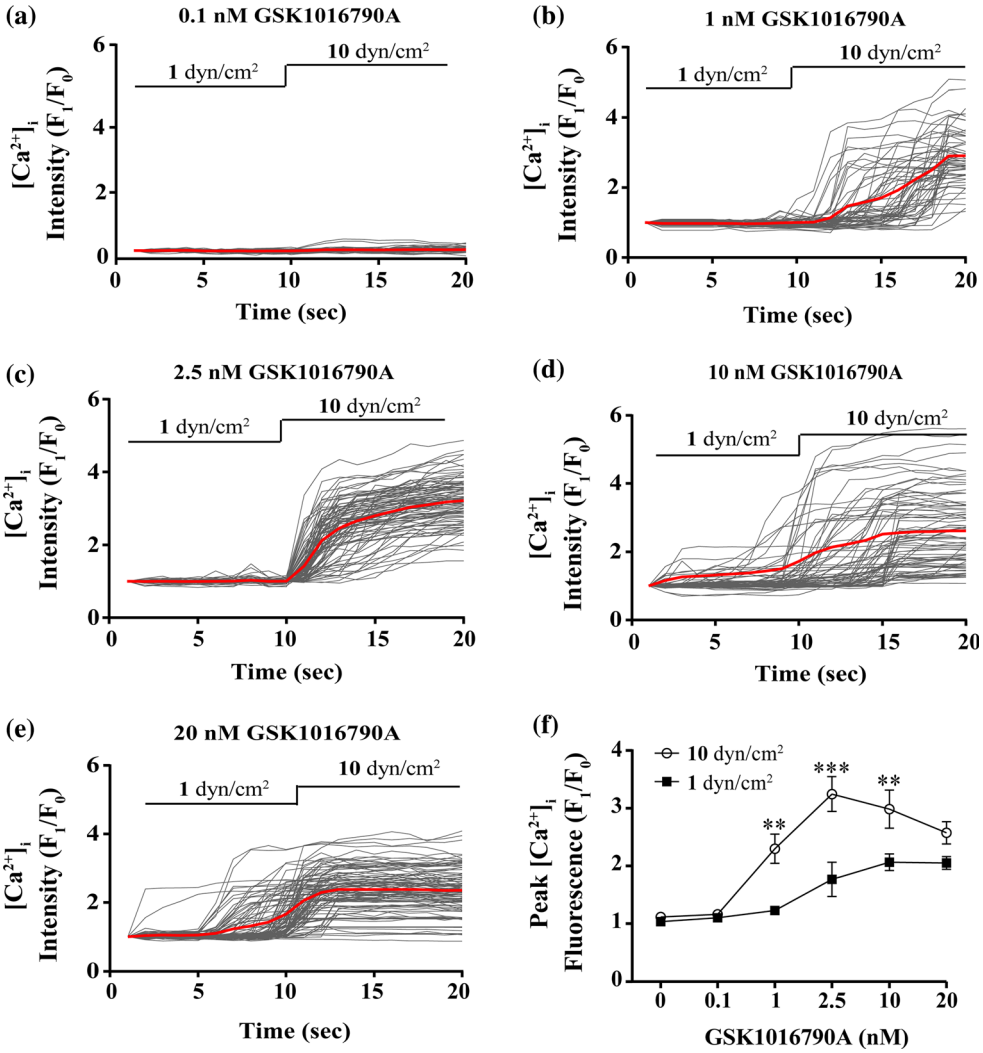

Fig. 1 Shear stress sensitises the response of HUVECs to GSK1016790A. **a–f** Increasing shear stress from 1 to 10 dyn/cm^2 sensitised the response of TRPV4 to its agonist GSK1016790A (0.1–20 nM). **a–e** *Grey lines* indicate single cell responses and the *red line* shows the average response. 40–70 cells were analysed in each experiments. **f** Peak amplitude of response ($n = 4$). 40 cells were analysed for each data point

Shear stress stimulation increases the surface density of TRPV4

Shear stress is reported to increase cell surface expression of Kir2.1 [32], Kv1.5 [33] and TRPM7 [34] ion channels. We hypothesised that shear stress sensitises the agonist effects of GSK1016790A by increasing the density of functional TRPV4 channels at the plasma membrane. To test this hypothesis, HEK293 cells were transiently transfected with a construct comprising the human TRPV4 cDNA with a C-terminal yellow fluorescent protein (YFP) fusion. Surface expression was measured using TIRFM. TIRFM revealed very motile puncta of TRPV4 at the plasma membrane with dynamic movement in the *x*/*y* axis (movie 1). Stimulation with a shear stress of 10 dyn/cm^2 resulted in a progressive increase of TRPV4-YFP evanescence field fluorescent (EFF), with a maximum of 21.73 ± 3.23-fold ($n = 7$) ($P < 0.001$) above the baseline (Fig. 2a–c, movie 2). To determine whether TRPV4-YFP fluorescent change resulted from trafficking of the channel

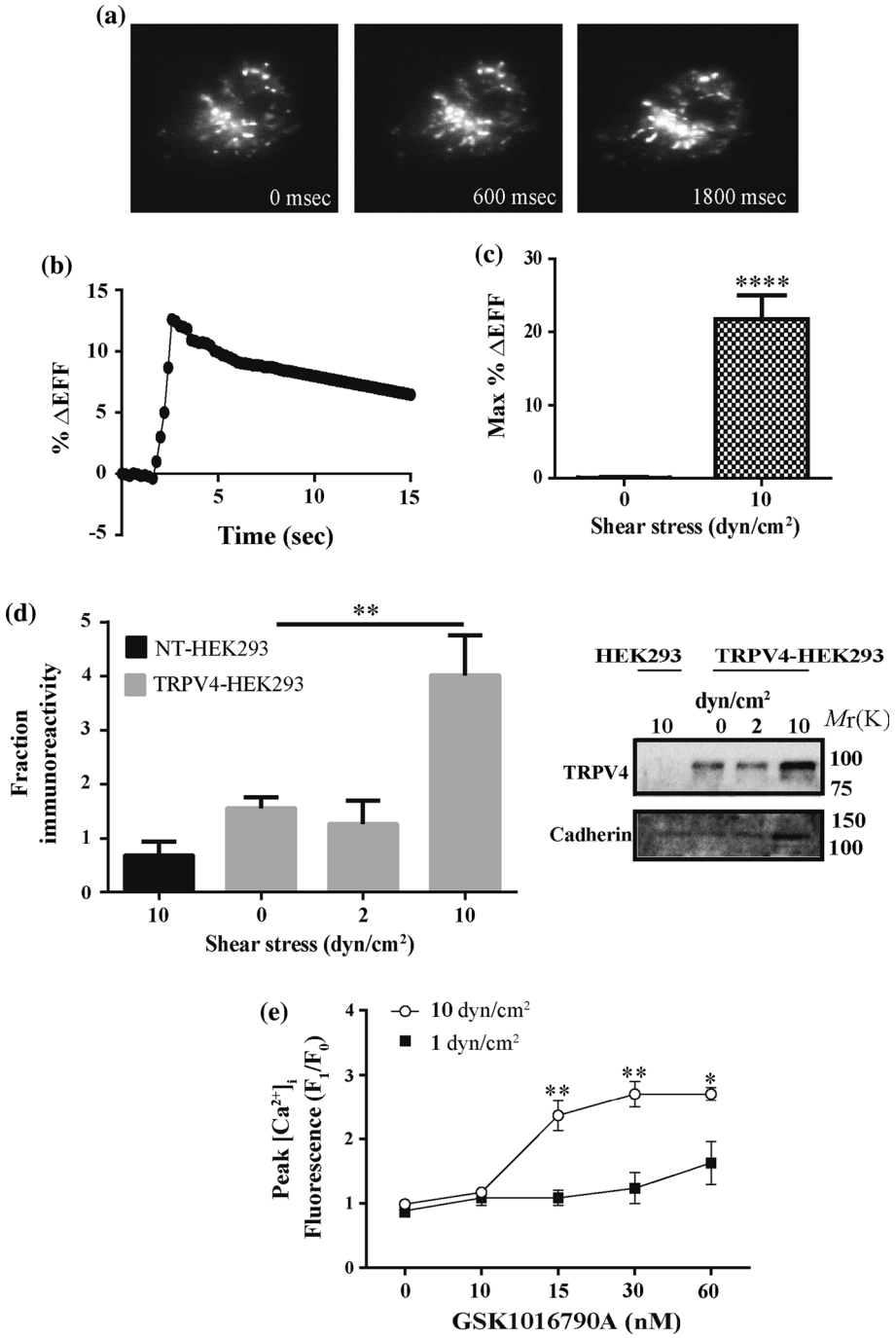

Fig. 2 Shear stress stimulates translocation of functional TRPV4 channels to the plasma membrane. **a** Representative TIRFM images recorded from a single HEK293 cell expressing TRPV4-YFP upon shear stress stimulation. **b** Quantitated time course of the increase in surface fluorescence in response to shear stress for the images shown in (**a**). **c** *Bar graph* showing maximum increase in the fluorescence before and after the application of shear stress ($n = 7$). **d** Cell surface biotinylation assay showing that shear stress increases the density of TRPV4 at the plasma membrane of TRPV4-HEK293 cells ($n = 6$). **e** Agonist sensitisation assay showing increasing shear stress from 2 to 10 dyn/cm^2 increases the response of TRPV4 to 0–60 nM of GSK1016790A (i = 4). Data are presented as the mean ± SEM, $^*P < 0.05$, $^{**}P < 0.001$ and $^{****}P < 0.0001$

rather than membrane motion or expansion of the cells under flow, we repeated the experiment using a fluorescent lysosome marker (Lysosome-RFP) and did not detect any global change in fluorescence after shear stress stimulation (movie 3). This suggests that the increase in fluorescence after shear stress is attributable to the transport of TRPV4-YFP molecules to the plasma membrane region.

TIRF microscopy is a valuable technique to visualise protein movement in the peri-plasmic region, but it does not define the expression of proteins within the plasma membrane. To confirm that increased evanescence fluorescence is due to trafficking of TRPV4 channels to the plasma membrane, we performed cell surface biotinylation assays. TRPV4-HEK293 cells were surface biotinylated and labelled TRPV4 quantified as described in "Methods". Confirming TIRFM results, shear stress of 10 dyn/cm^2 increased biotinylated TRPV4 by 2.46 ± 0.66-fold ($n = 6$) ($P < 0.01$) over basal levels (Fig. 2d).

To further investigate how shear stress sensitises the TRPV4 channel response to its agonist (GSK1016790A), TRPV4-HEK cells were exposed to shear stress of 1 or 10 dyn/cm^2 in the presence of graded concentrations of GSK1016790A (10–60 nM) and changes in $[Ca^{2+}]_i$ were measured. At GSK1016790A concentrations of 10 nM or less, shear stress did not induce any changes in $[Ca^{2+}]_i$. However, at higher concentrations GSK1016790A sensitised the response of TRPV4 in a similar manner to that seen in HUVECs (Fig. 2e). Together, these experiments indicate shear stress stimulates the recruitment and accumulation of functional TRPV4 channels at the plasma membrane and that agonist sensitisation is more sensitive in HUVECs than in TRPV4-HEK293 cells.

TRPV4 Tyrosine 110 is important for the shear stress TRPV4 activation and trafficking

Phosphorylation of TRPV4 tyrosine residue Y110 and Y805 has previously been demonstrated, by mass spectrometry and a TRPV4 Y110F mutation inhibited sensitisation of TRPV4 to shear stress and hypo-osmotic shock [29]. We used HEK293 TRPV4 Y110F cells [30] to further evaluate the functional role of Y110 in shear stress-induced agonist sensitisation and trafficking of TRPV4. Using selective reaction monitoring mass spectrometry, we found shear stress induces the phosphorylation of TRPV4 at the Y110 residue but did not change the phosphorylation of Y805, S162 or S824 (Fig. 3a; Supplementary Fig. 1a.). We therefore further investigated the importance of Y110 in shear stress-induced TRPV4 trafficking.

We found that the Y110F mutation did not block sensitisation of the specific agonist, GSK1016790A (Fig. 3b).

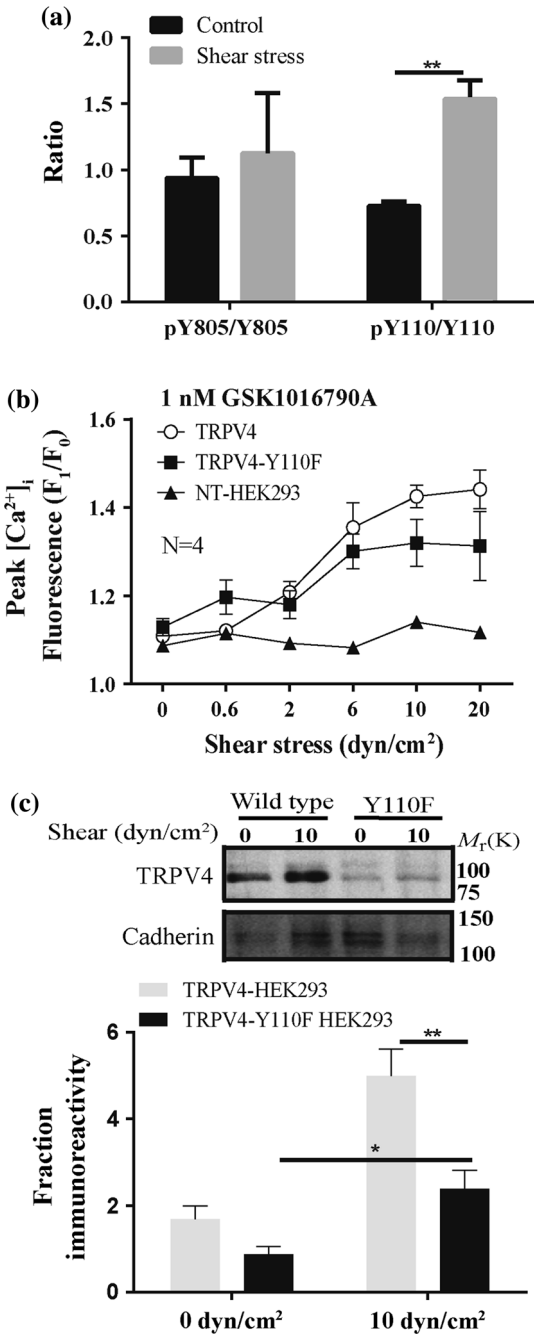

Fig. 3 Tyrosine 110 (Y110) is not important for the shear stress-dependent translocation of TRPV4. **a** SRM assay detecting TRPV4 Y110 and Y805 phosphorylation. *Graph* shows TRPV4 Y110 and Y805 phosphorylation stoichiometries in control and shear stress-induced cells. Peak area ratios (endogenous/synthetic tryptic peptides) are normalised using the median value and the ratios for the phosphopeptides are divided by the ratios for the unmodified peptide ($n = 4$). **b** The Y110F mutation did change the sensitisation effect of shear stress on TRPV4 response to its specific agonist GSK1016790A ($n = 4$). **c** Cell surface biotinylation assay. Plasma membrane density of TRPV4 Y110F expressed in HEK293 cells is reduced, as is reduced shear-induced translocation of TRPV4 channels ($n = 6$). Data are presented as the mean ± SEM, *$P < 0.05$ and **$P < 0.01$

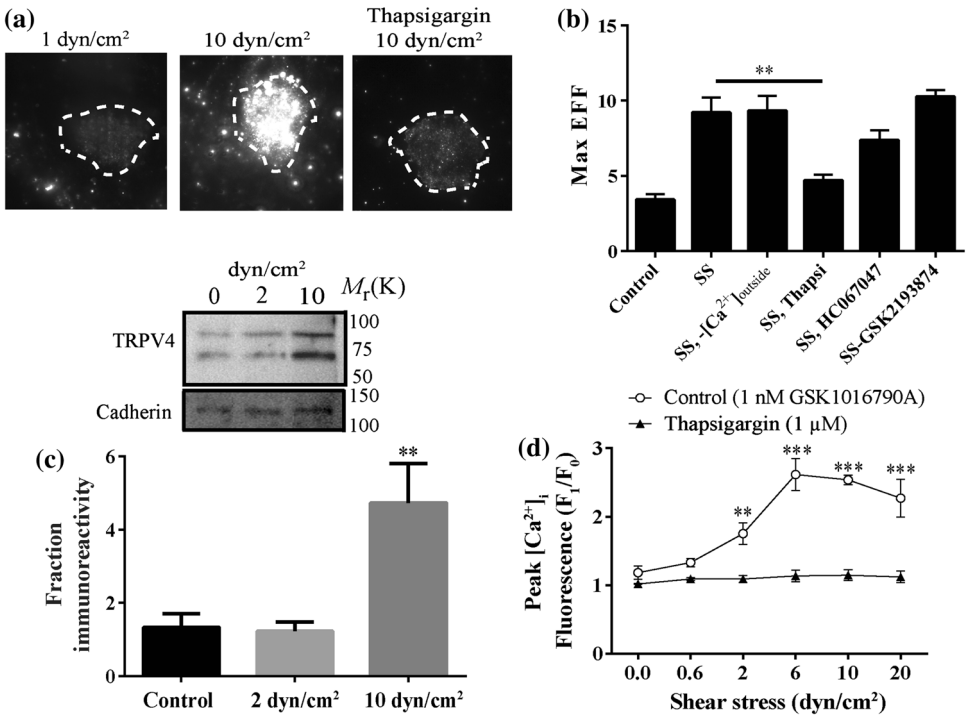

Fig. 4 Shear-induced trafficking of TRPV4 channels is dependent on release of Ca^{2+} from intracellular stores in HUVECs. **a**, **b** Evanescence field microscopy shows pre-treatment with thapsigargin (Thapsi) blocked the increase in cell surface EEF density of TRPV4 channels post-shear-stress (SS) stimulation. HUVECs were treated with shear stress levels of 1–10 dyn/cm^2 for 30 s, with or without 30 min pre-treatment with HC067047 (100 nM), GSK2198374 (100 nM), thapsigargin (1 µM) or in the absence of Ca^{2+}(-$[Ca^{2+}]_o$). Samples were fixed and stained for TRPV4 ($n = 4$ channels, 10 cells were analysed in each replicate). **c** Cell surface biotinylation assays showing shear stress stimulation increases the surface density of TRPV4 dependent on the magnitude of shear ($n = 6$). **d** Depletion of Ca^{2+} from intracellular stores inhibited the shear stress-dependent sensitisation of the response to GSK1016790A ($n = 4$). Data are presented as the mean ± SEM, $^{**}P < 0.01$, $^{***}P < 0.001$

Notably, the Y110F mutation did not change the TRPV4 response to GSK1016790A in the absence of shear stress (Supplementary Fig. 1b).

Western blotting of whole cell lysates revealed that in HEK293 cells, expression of the TRPV4 Y110F was 4.8 ± 0.6-fold higher than the wild-type TRPV4 construct ($n = 4$, $P < 0.01$) (Supplementary Fig. 1c). However, when normalised to endogenously expressed cadherin levels, we found the surface density of Y110F, as measured by biotinylation, was less than that of wild-type TRPV4 (Fig. 3c). The mutant also exhibited increase in cell surface expression following stimulation by a shear stress of 10 dyn/cm^2 [1.6 ± 0.6-fold increase ($P < 0.05$)] that was less than wild type [2.6 ± 0.6-fold less ($P < 0.01$)].

These data demonstrate that shear stress increases the phosphorylation of Y110 and is necessary for the TRPV4 Ca^{2+} response to shear stress. However, Y110 phosphorylation is not necessary for the shear-induced translocation of TRPV4 channels to the plasma membrane, or for TRPV4 response to its selective agonist, as mutation to phenylalanine neither blocked the trafficking of TRPV4 upon shear stress stimulation nor reduced the TRPV4 response to GSK1016790A. This suggests that shear-dependant translocation is controlled through a distinct mechanism to channel opening.

Release of calcium from intracellular stores is necessary for shear stress-dependent increase in TRPV4 cell surface density

To determine whether intracellular Ca^{2+} influx plays a role in shear stress-dependent trafficking of TRPV4 to the plasma membrane, we removed Ca^{2+} from the buffer solution or blocked TRPV4 with its selective antagonists, HC067047 [30] or GSK2198374 [35]. We then measured TRPV4 density at the plasma membrane using TIRF microscopy.

Shear stress stimulation increased the density of TRPV4 in the TIRFM field of view from 3.4 ± 0.3 to 9.2 ± 0.9-fold ($n = 4$) ($P < 0.01$) (Fig. 4a, b) above the base-line levels. This was confirmed by biotinylation assays, where a shear stress of 10 dyn/cm^2 increased the density of biotinylated TRPV4 by 3.4 ± 1 fold ($n = 6$) ($P < 0.01$) compared to control (Fig. 4c). Furthermore, chelation of

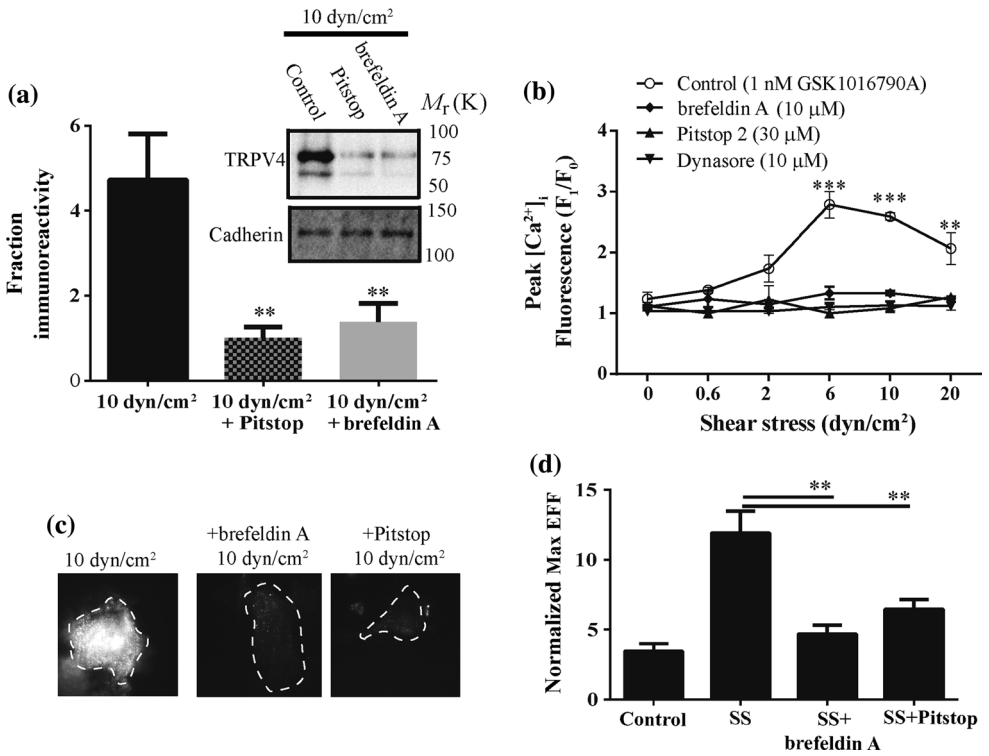

Fig. 5 Shear stress induces exocytosis of the TRPV4 channels through a clathrin-mediated pathway. **a** Cell surface biotinylation assay shows that inhibition of protein transport from ER to Golgi or clathrin with brefeldin A or Pitstop, respectively, reduces surface density of TRPV4 post-shear-stress stimulation ($n = 5$). **b** Sensitisation assay showing that 30-min pre-treatment with brefeldin A, Pitstop or dynamin blocked the sensitisation effect of shear stress on TRPV4 response to GSK1016790A (1 nM). **c**, **d** Evanescence field microscopy shows pre-treatment with brefeldin A (10 μM) for 12 h to inhibit protein transport from the ER to Golgi, or Pitstop (30 μM) for 10 min to block clathrin-mediated exocytosis, blocked the EEF density of TRPV4 channels post-shear-stress stimulation ($n = 3$) channels, 10 cells have been analysed in each. Data are the mean ± SEM, $^{**}P < 0.01$, $^{***}P < 0.001$

extracellular calcium with EGTA did not affect the shear-induced trafficking of TRPV4 in either HUVECs or TRPV4-HEK293 cells, nor did HC067047 or GSK2198374 (Fig. 4a, b).

We tested if release of Ca^{2+} from intracellular stores contributed to shear stress-dependent trafficking. Intracellular stores of Ca^{2+} were depleted using 30 min thapsigargin pre-treatment and the effects on TRPV4 trafficking were assessed.

Depletion of intracellular Ca^{2+} stores with thapsigargin (1 μM) abolished shear stress-dependent sensitisation of GSK1016790A responses ($P < 0.01$) (Fig. 4d). Thapsigargin also reduced the effect of shear stress to enhance TRPV4 surface density from 9.2 ± 0.9 fold ($n = 4$) to 4.6 ± 0.4 fold ($n = 4$) ($P < 0.01$) (Fig. 4a, b).

Shear stress stimulates channel exocytosis through a clathrin-dependent pathway that requires intact actin

To identify the pathways that are involved in trafficking of TRPV4 channels upon stimulation by shear stress, we first blocked protein export from endoplasmic reticulum (ER) to Golgi using brefeldin A [36]. Brefeldin A treatment blocked the sensitisation of shear stress effects on TRPV4 channel response to GSK1016790A (Fig. 5b).

Furthermore, cell surface biotinylation assays revealed that pre-treatment with brefeldin A, significantly reduced shear-induced trafficking of TRPV4 channels to the plasma membrane by 3.3 ± 0.8-fold ($P < 0.01$) (Fig. 5a) suggesting it blocks the trafficking of functional channels to the plasma membrane.

The trans-Golgi network (TGN) is a major secretory pathway responsible for sorting of newly synthesised protein to different subcellular compartments [37]. From the TGN, protein cargo can be transferred directly to the cell membrane or they can transfer through the trans-endosomal routs and recycling endosomes [38]. Clathrin has recently been identified an accessory protein for transfer between the TGN and plasma membrane by direct exocytosis through the endosomal pathway [37]. Dynamin has been implicated as a key player in membrane fission at the TGN [39]. We found that pre-treatment with Pitstop, a clathrin inhibitor, reduced the shear stress-induced

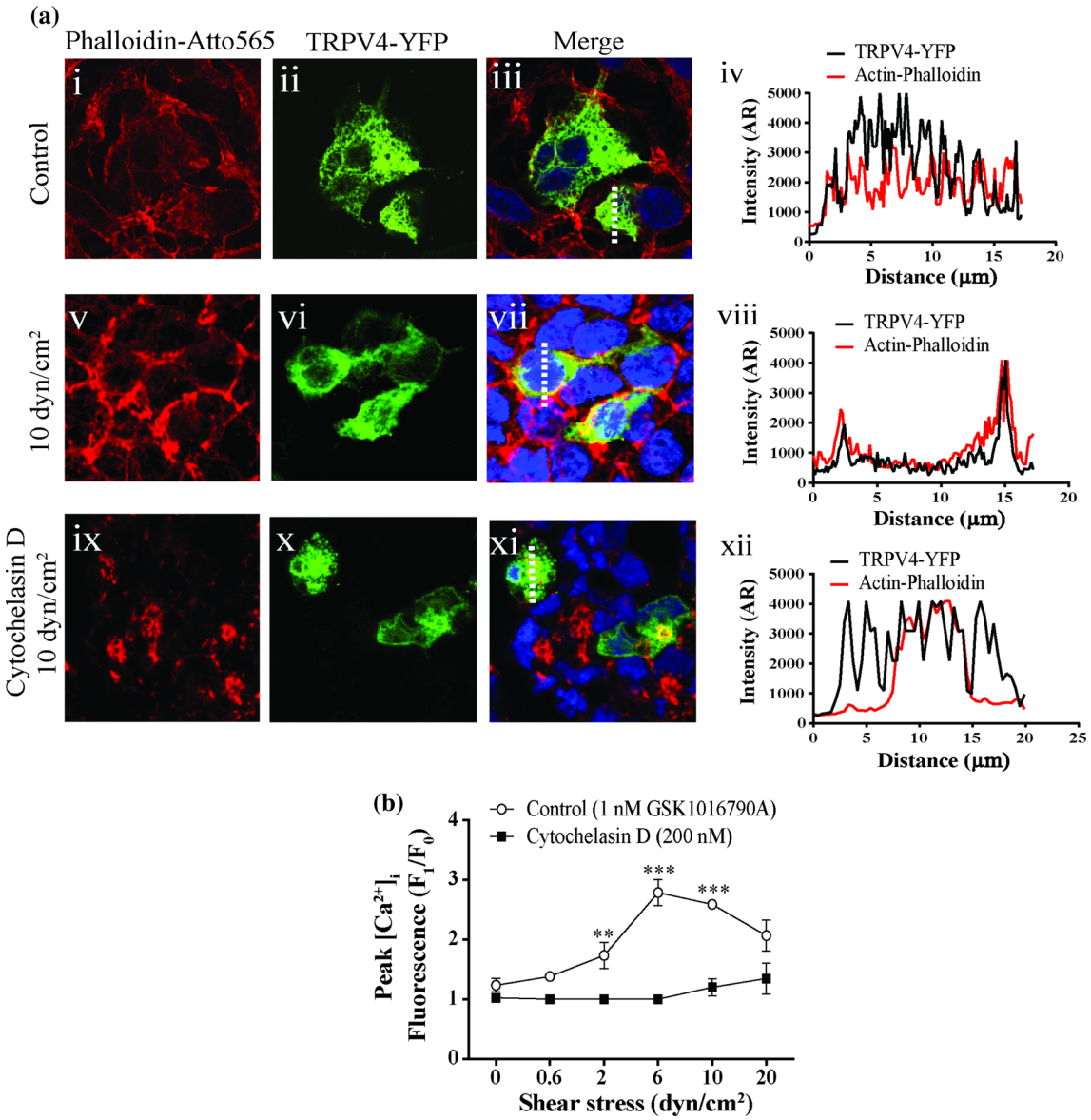

Fig. 6 Shear stress induces actin and TRPV4 movement to the plasma membrane. **a** Representative confocal images of HEK293 cells, showing actin stained with Atto 565-phalloidin (*i*, *v*, *ix*) and TRPV4-YFP (*ii*, *vi*, *vii*) and extent of colocalisation (*iii*, *vii*, *xi*) at steady state or in the presence of a shear stress of 10 dyn/cm^2 (with/without cytochalasin D treatment). Graphs *iv*, *viii* and *xii* show the fluorescence intensity profiles, indicating the extent of TRPV4 and actin colocalisation (as determined along the area marked by the *dashed white lines*). **b** Pre-treatment with cytochalasin D (200 nM) for 30 min abolishes the sensitisation effect of shear stress on TRPV4 response to GSK1016790A (1 nM) ($n = 4$). Data are presented as the mean ± SEM, $^{**}P < 0.01$, $^{***}P < 0.001$

trafficking of TRPV4 channels to the cell membrane by 3.7 ± 0.8-fold ($P < 0.01$) (Fig. 5c, d) and also blocked the shear stress sensitisation effects with agonist treatment (Fig. 5b). Similarly, pre-treatment with the dynamin inhibitor dynasore hydrate [40], reduced the sensitisation effect of shear stress on agonist activation of TRPV4 (Fig. 5b).

Actin dynamics are postulated to play a key role in exocytosis of post-Golgi vesicles [41] and TRPV4 is known to have a functional interaction with actin cytoskeleton [42]. Pre-treatment of HUVECs with cytochalasin D abolished shear-induced sensitisation of TRPV4 response to GSK1016790A (Fig. 6b) in a similar manner to that observed in HEK293 cells (data not shown). None of the treatments reported here, altered the potency or efficacy of GSK1016790A response (Supplementary Fig. 2a).

To examine the role of actin dynamics in exocytosis of TRPV4 channels, we destabilised the actin network with cytochalasin D. In the absence of shear stress, YFP-TRPV4 was localised to both cytoplasm and plasma membranes.

F-actin was present in these cells as shown by Atto 565-phalloidin staining (Fig. 6a i–iv). After stimulation with shear, both TRPV4-YFP and actin localised to the plasma membrane (Fig. 6a v–viii). In the merged images, these proteins colocalised at both cytoplasm and plasma membrane. After treatment with cytochalasin D, the organisation of actin was dramatically altered; however, merged images showed the colocalisation of actin and TRPV4 in both unstimulated and shear stimulated cells (Fig. 6a ix–xii; supplementary Fig. 2b).

Phosphorylation by PKA but not PKC and PKG is important in shear stress-induced translocation of TRPV4

Phosphorylation of TRPV4 by protein kinase C (PKC) and protein kinase A (PKA) has been reported to sensitise TRPV4 [43]. Activation of PKC-dependent pathways sensitises TRPV4 to shear stress, while PKA-dependent pathways are involved in translocation and trafficking of TRPV4 to the apical membrane in the distal nephron [44].

Here, we tested the effect of PKC, PKA and PKG-dependent pathways on TRPV4 translocation to the plasma membrane upon shear stress stimulation. Pre-treatment with the PKC inhibitor, bisindolylmaleimide I (BIM-1) (200 nM) and the PKG inhibitor, KT 5823 (2 μM) had no effect on TRPV4 response to its agonist, GSK1016790A and did not change the surface density of TRPV4, as measured by TIRFM (Fig. 7a). However, the PKA inhibitors, H89 (200 nM) and PKI (10 μM) ablated the effect of shear stress on TRPV4 response to its agonist, GSK1016790A (Fig. 7b). Further, the selective PKA inhibitors, H89 (200 nM) significantly reduced the density of TRPV4 channels at the plasma membrane by 2 ± 0.8-fold ($P < 0.01$) compared to the shear stress control group (Fig. 7a). Cell surface biotinylation assay confirmed the TIRFM data (Supplementary 4).

Shear stress-induced translocation of TRPV4 is mediated by ILK/Akt signalling

Integrins are known mechano-transducers that mediate signalling events in vascular endothelial cells by connecting the extracellular matrix with intracellular signalling pathways [45]. Integrin-linked kinase (ILK) is a serine/threonine kinase that binds to the cytoplasmic domains of β1, β2 and β3 Integrin subunits [46]. We examined the involvement of ILK in response to shear stress using the ILK inhibitor, Cpd22 [47]. HUVECs were grown on coverslips and subjected to a shear stress of 10 dyn/cm^2 in the presence or absence of the ILK inhibitor (200 nM). Measuring the surface density of TRPV4 using the biotinylation

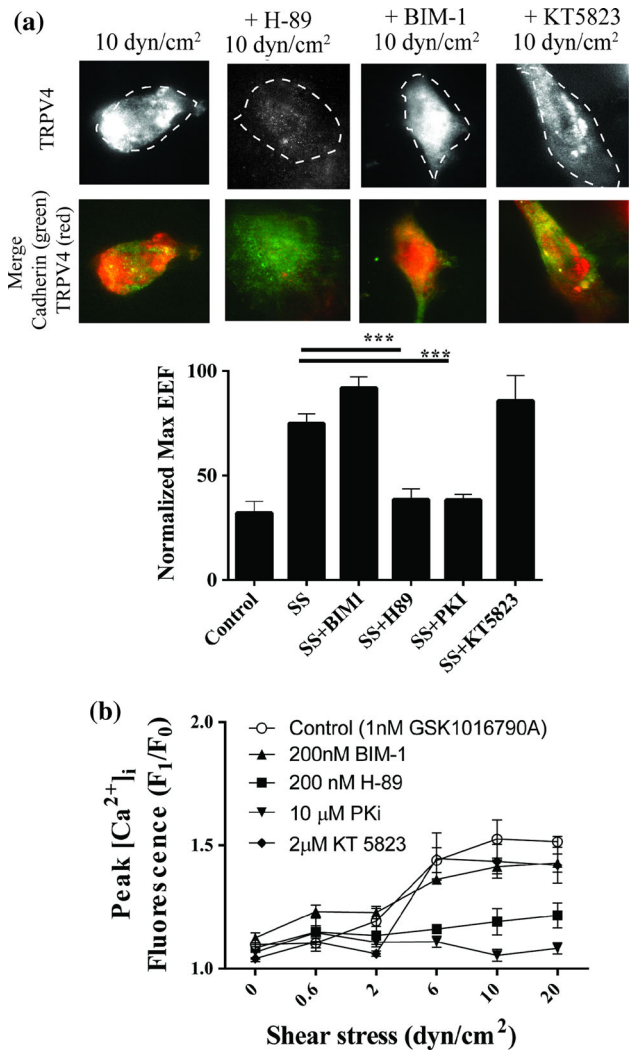

Fig. 7 Shear-induced trafficking of TRPV4 channels is PKA dependent. **a** Evanescence field microscopy shows that pre-treatment with the inhibitor of PKA (H-89, 200 nM), reduces the EEF density of TRPV4 channels post-shear stress (*red channel*) (SS) stimulation compared to the membrane protein, cadherin (*green channel*), $n = 3$ and 10 cells have been analysed in each experiment. **b** Agonist sensitisation assay showing that 30 min pre-treatment with inhibitors of PKA, (H-89, 200 nM) and (PKI, 10 μM) but not the PKC inhibitor (BIM-1, 200 nM) and PKG inhibitor (KT 5823, 2 μM) blocked the sensitisation effect of shear stress on TRPV4 response to GSK1016790A, $n = 4$. Data is presented as the mean ± SEM, $^{***}P < 0.001$

assay, showed that pre-treatment with Cpd22 reduced the density of TRPV4 at the plasma membrane by 3.6 ± 0.7-fold, $P < 0.001$ ($n = 6$). Inhibition of ILK also reduced the sensitisation effect of shear stress on TRPV4 response to GSK1016790A (Fig. 8a, b). It has been suggested that αvβ3 integrin, PECAM1, VE-cadherin and VEGFR2 are important in the endothelial response to shear and signal through Akt [48, 49]. However, pre-treatment with the β1 and β3 integrin-selective toxin, echistatin did not affect the

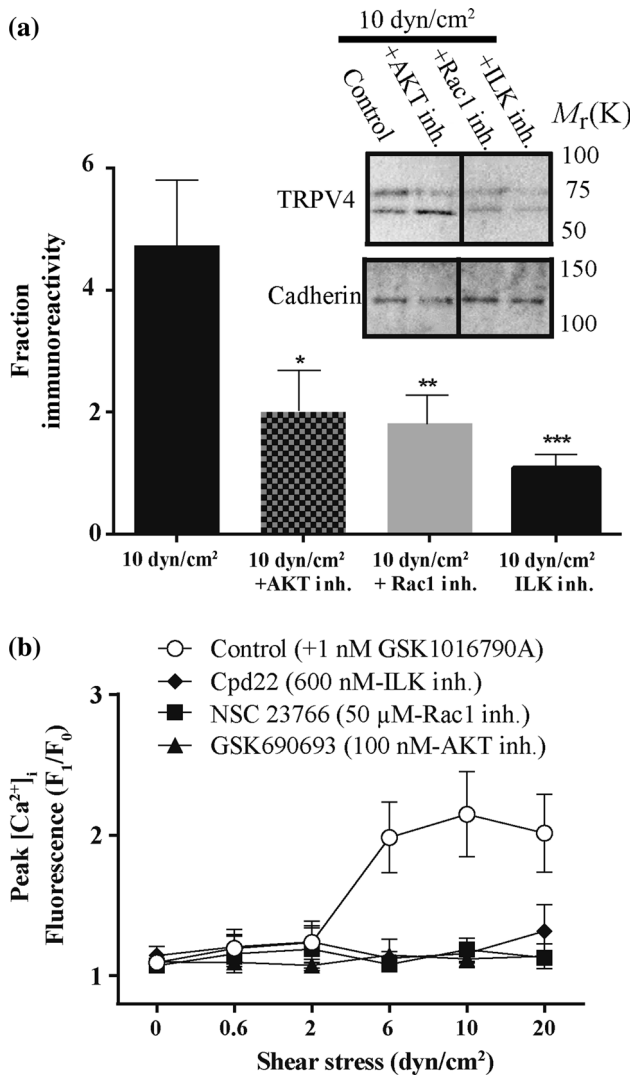

Fig. 8 ILK and Akt signalling pathways are necessary for shear-induced translocation of TRPV4 to the plasma membrane. **a** Cell surface biotinylation and **b** sensitisation assay of HUVECs pre-treated with ILK inhibitor (Cpd22, 600 nM), Rac1 inhibitor (NSC23766, 50 µM) or Akt inhibitor (GSK690693, 100 nM) for 30 min in presence of a shear stress of 10 dyn/cm^2. **a** $n = 5$ **b** $n = 4$. Data are given as the mean ± SEM, *$P < 0.05$, **$P < 0.01$, ***$P < 0.001$

sensitisation effect of shear on the TRPV4 response to GSK1016790A.

In endothelial cells, ILK has been implicated in activation of the Rho family GTPase, Rac1, which modulates signal transduction and regulates actin cytoskeleton dynamics in response to matrix interaction with Integrins and other membrane proteins [50]. We treated HUVECs with the Rac1 inhibitor, NCS 23766 (50 µM) [51], before applying a shear stress of 10 dyn/cm^2. NCS 23766 impaired the sensitisation effect of shear stress on TRPV4 response to GSK1016790A and also reduced the surface expression of TRPV4 channels by 2.9 ± 0.7 fold, $P < 0.01$ ($n = 6$), compared to the control group (Fig. 8a, b).

The serine/threonine kinase Akt plays a key role in integrin mediated mechanotransduction. After pre-treated with the Akt inhibitor, GSK690693 (100 nM), shear stress no longer sensitise the response of TRPV4 to its agonist and did not induced trafficking of TRPV4 to the cell membrane (2.7 ± 0.7 fold, $P < 0.05$ ($n = 5$), compared to the control group (Fig. 8a, b). These results indicate that shear stress is transduced via the activation of ILK/Akt to trigger the release of TRPV4 channels to the plasma membrane and this likely involves an as yet unidentified integrin.

Discussion

In this study, we investigate the mechanism by which TRPV4 is sensitised and opens in response to shear stress (Fig. 7). As reported before by us and others, TRPV4 is an indirectly activated high-threshold mechanosensitive Ca^{2+} permeable channel which is opened by shear stress in some cells [52]. However, the molecular basis of this mechanosensitivity is not understood.

Here, we show that in HUVECs and in TRPV4 transfected HEK293 cells, shear stress stimulates an increase of $[Ca^{2+}]_i$, which is mostly due to influx of calcium through TRPV4, with the remainder coming from intracellular stores. Using TIRF microscopy and cell surface biotinylation, we demonstrated that shear stress triggers translocation of TRPV4 channels to the plasma membrane within seconds of treatment. This process is independent of Ca^{2+} influx through TRPV4 but requires release of Ca^{2+} from intracellular stores. Our data are consistent with shear stress-induced TRPV4 exocytosis.

Exocytosis of intracellular vesicular cargo is often divided into regulated or constitutive pathways. Constitutive exocytosis regulates trafficking of membrane proteins and is a rapid process, in which post-Golgi vesicles fuse to the cell membrane and release their cargo, in a mechanism that is independent of calcium influx [53]. Regulated exocytosis controls the delivery of secretory products and is triggered by the activation of a signalling cascade which may include calcium influx [54]. Vesicle movement from the ER to the intra-Golgi network is controlled by the release of calcium from intracellular stores [55, 56].

Our data show that shear-induced elevation of $[Ca^{2+}]_i$ and trafficking of the TRPV4 channel to the cell membrane are both inhibited by depletion of intracellular Ca^{2+} stores with thapsigargin, while removal of Ca^{2+} from the extracellular buffer does not show any effect on trafficking. This data is consistent with previous reports showing that calcium release from intracellular stores plays a role in endothelial cell Ca^{2+} response to shear stress [57]. It is

known that release of calcium from intracellular stores is due to activation of inositol triphosphate receptors by inositol 1,4,5-triphosphate (IP_3) [58]; however, the molecular mechanism by which intracellular calcium release affects trafficking of TRPV4 is not known.

Post-Golgi vesicle exocytosis is regulated by dynamin, which supports the scission of clathrin-coated vesicles from trans-Golgi network [59]. Clathrin performs a critical function in sorting of transport cargo and ensuring correct compartmentalisation via the trans-Golgi network. Clathrin sorts vesicles to the endosomal compartment where dynamin and other GTPases together with cytoskeletal proteins such as actin, direct vesicle fusion to the cell membrane [39]. Our experiments demonstrate the dependence of TRPV4 channel trafficking on a clathrin- and dynamin-mediated pathway of exocytosis. Moreover, the inhibition of shear stress-dependent translocation of TRPV4 by brefeldin A suggests that translocation also requires transport from the ER to the Golgi network.

The cytoskeleton regulates many of cellular functions involving TRPV4, such as regulation of cell volume [60, 61] and mechanotransduction [62]. In our experiments, TRPV4 shows colocalisation with actin, regardless of treatments applied. This is consistent with a previous report showing that actin binds to both monomeric and polymeric TRPV4 in a neuronal cell line [63]. We find that shear-induced agonist sensitisation and exocytosis of TRPV4 is dependent on the formation of actin filaments and the Rho-GTPase Rac1. Rho GTPases have been shown to play an important role in cytoskeleton rearrangement as well as vesicular transport during exocytosis [64, 65]. Actin remodelling following the activation of Rho family GTPase has previously been shown to regulate trafficking of TRPV4 to the plasma membrane [66].

Integrins and the extracellular matrix have been implicated in mechanotransduction in endothelial cells [67], vascular smooth muscle cells [68] and neurons [69]. Mechanical stretch of capillary endothelial cells has been demonstrated to activate TRPV4 channels through an integrin signalling pathway [70]. Activation of αvβ3 integrins is necessary for the vascular endothelial cell response to shear stress [48]. Integrins provide a physical link between extracellular matrix and cytoskeleton and help stimulation of intracellular signalling through focal-adhesion kinase (FAK) and other pathway components. ILK is a serine/threonine kinase and scaffolding protein that transduces integrin signals [71]. ILK binds directly to the cytoplasmic domain of β1 and β3 integrins and indirectly to the actin and is present in focal adhesions [72, 73]. Several in vitro studies have suggested that ILK transfers key signals through phosphorylation of Akt [74]. The physical interaction of PKA with phosphorylated form of Akt is necessary for Akt signalling [75]. Shear stress is reported to activate endothelial NO synthesis (eNOS) via PKA and Akt pathways and NO can play a regulatory role in exocytosis, by nitrosylation of dynamin to increase the rates of dynamin assembly and dynamin-dependent exocytosis and endocytosis [76]. This suggests a possible mechanistic link between shear stress and TRPV4 exocytosis. We propose to test the effect of the NOS inhibitor L-NAME on shear-dependent translocation of TRPV4 in the future.

In addition to the localisation of ILK at integrin sites, it is present in other subcellular regions and compartments, where it plays integrin independent roles. For example, ILK is involved in connecting microtubules to the cortical actin networks via scaffolding proteins, to connect the complex to integrin adhesion sites. Thus, the connection of these networks by ILK may play a role in exocytosis of different membrane proteins [77].

Interestingly echistatin, an inhibitor of αvβ3 and α5β1 integrin signalling [78] has no effect on shear-induced trafficking of TRPV4, whereas inhibitors of ILK, Akt and PKA completely block its trafficking. These data suggest this process is either independent of integrins or dependent on integrins other than αvβ3 or α5β1. Further, we found that this trafficking is independent of TRPV4 opening.

Our results show that inhibition of either ILK or Akt signalling pathways impairs the shear- induced translocation of TRPV4 channels to the plasma membrane, implicating this signalling pathway in a regulatory role for TRPV4-mediated mechanotransduction.

Our results suggest that increase at the density of functional TRPV4 in the plasma membrane results from recruitment of channels in intracellular vesicles through the process of constitutive exocytosis (Fig. 9). This pathway is regulated through integrins and extracellular matrix. The findings reported here represent a novel mechanism for TRPV4 regulation in response to mechanical stress in vascular endothelial cells and other mechanosensitive cells.

TRPV4 expression is not limited to vascular endothelium but it is also expressed in epithelial cells, kidney cells, chondrocytes and sensory and motor neurons [79–81]. For example, it has been shown that TRPV4 is differentially distributed along different vascular segments of kidney and plays distinct vasoregulatory functions to other TRP channels that are expressed in kidney [82–84]. TRPV4 is also involved in developmental bone and joint diseases, and in different pathologies including hypertension, muscular dystrophy and cancer [5–7].

It has been shown that in mesenteric arteries, Ca^{2+} influx through discrete clusters of endothelial TRPV4 ion channels

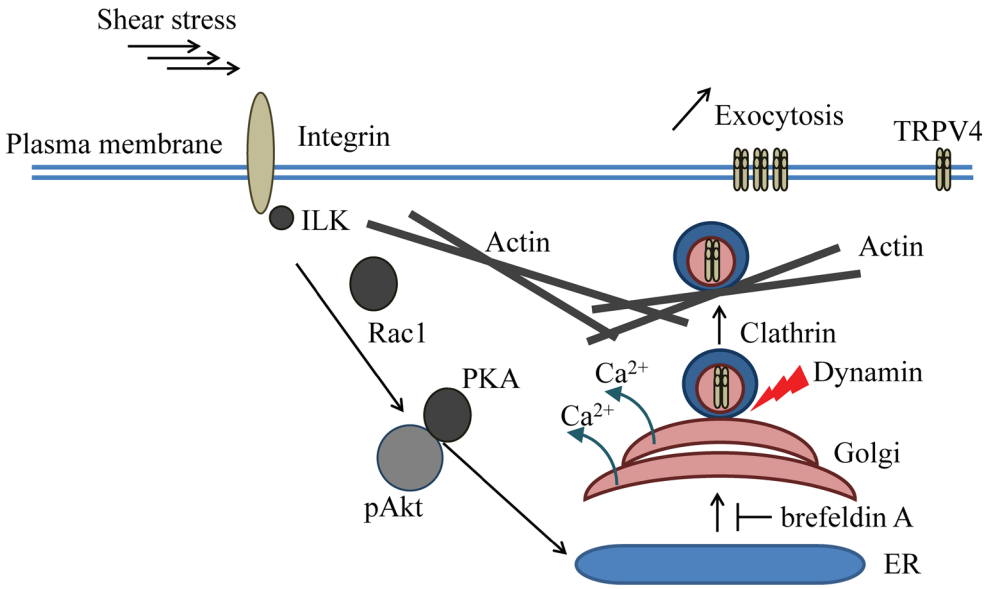

Fig. 9 Schematic presentation of TRPV4 recruitment to the plasma membrane in response to shear stress. Increase in shear stress is sensed by integrins that convey the signals through the ILK and Akt to ER and Golgi. This causes the release of TRPV4 channels to the plasma membrane which requires an intact actin cytoskeleton and is dependent on the release of calcium from intracellular stores. This mechanotransduction pathway is likely to influence the endothelial cell responses to TRPV4-specific agonist

regulates relaxation of smooth muscle cells and such relaxation causing dilation is impaired during hypertension [83, 84]. Therefore, TRPV4 regulation through regulation of membrane expression is likely to be relevant to diseases where mechanical signalling is altered and it may be possible to target this process for therapeutic benefit.

Acknowledgments We thank Dr. Suzanne Rogers and Professor Nigel Bunnett for the critical reading of the manuscript. This research was supported by project funding from the Australian National Health and Medical Research Council (project Grant 1046860 to PMc).

References

1. Delmas P, Hao J, Rodat-Despoix L (2011) Molecular mechanisms of mechanotransduction in mammalian sensory neurons. Nat Rev Neurosci 12(3):139–153. doi:10.1038/nrn2993
2. Yashiro K, Shiratori H, Hamada H (2007) Haemodynamics determined by a genetic programme govern asymmetric development of the aortic arch. Nature 450(7167):285–288. doi:10.1038/nature06254
3. Ranade SS, Qiu Z, Woo S-H, Hur SS, Murthy SE, Cahalan SM, Xu J, Mathur J, Bandell M, Coste B, Li Y-SJ, Chien S, Patapoutian A (2014) Piezo1, a mechanically activated ion channel, is required for vascular development in mice. Proc Natl Acad Sci USA 111(28):10347–10352. doi:10.1073/pnas.1409233111
4. Orr AW, Helmke BP, Blackman BR, Schwartz MA (2006) Mechanisms of mechanotransduction. Dev Cell 10(1):11–20. doi:10.1016/j.devcel.2005.12.006
5. Hahn C, Schwartz MA (2009) Mechanotransduction in vascular physiology and atherogenesis. Nat Rev Mol Cell Biol 10(1):53–62. doi:10.1038/nrm2596
6. Huang S, Ingber DE (2005) Cell tension, matrix mechanics, and cancer development. Cancer Cell 8(3):175–176. doi:10.1016/j.ccr.2005.08.009
7. Lansman JB, Franco-Obregon A (2006) Mechanosensitive ion channels in skeletal muscle: a link in the membrane pathology of muscular dystrophy. Clin Exp Pharmacol Physiol 33(7):649–656. doi:10.1111/j.1440-1681.2006.04393.x
8. Discher DE, Janmey P, Wang YL (2005) Tissue cells feel and respond to the stiffness of their substrate. Science 310(5751):1139–1143. doi:10.1126/science.1116995
9. Martinac B (2004) Mechanosensitive ion channels: molecules of mechanotransduction. J Cell Sci 117(12):2449–2460. doi:10.1242/jcs.01232
10. Mammoto A, Mammoto T, Ingber DE (2008) Rho signaling and mechanical control of vascular development. Curr Opin Hematol 15(3):228–234. doi:10.1097/MOH.0b013e3282fa7445
11. Coste B, Xiao B, Santos JS, Syeda R, Grandl J, Spencer KS, Kim SE, Schmidt M, Mathur J, Dubin AE, Montal M, Patapoutian A (2012) Piezo proteins are pore-forming subunits of mechanically activated channels. Nature 483(7388):176–181. doi:10.1038/nature10812
12. Wehrle-Haller B (2007) Analysis of integrin dynamics by fluorescence recovery after photobleaching. Methods Mol Biol (Clifton, NJ) 370:173–202
13. Hu K, Ji L, Applegate KT, Danuser G, Waterman-Storer CM (2007) Differential transmission of actin motion within focal adhesions. Science 315(5808):111–115. doi:10.1126/science.1135085
14. Brown CM, Hebert B, Kolin DL, Zareno J, Whitmore L, Horwitz AR, Wiseman PW (2006) Probing the integrin-actin linkage using high-resolution protein velocity mapping. J Cell Sci 119(24):5204–5214. doi:10.1242/jcs.03321
15. Hoffman BD, Grashoff C, Schwartz MA (2011) Dynamic molecular processes mediate cellular mechanotransduction. Nature 475(7356):316–323. doi:10.1038/nature10316

16. Jackson WF (2000) Ion channels and vascular tone. Hypertension 35(1):173–178
17. Nilius B, Vriens J, Prenen J, Droogmans G, Voets T (2004) TRPV4 calcium entry channel: a paradigm for gating diversity. Am J Physiol Cell Physiol 286(2):C195–C205. doi:10.1152/ajpcell.00365.2003
18. Liedtke W, Kim C (2005) Functionality of the TRPV subfamily of TRP ion channels: add mechano-TRP and osmo-TRP to the lexicon! Cell Mol Life Sci 62(24):2985–3001. doi:10.1007/s00018-005-5181-5
19. Mendoza SA, Fang J, Gutterman DD, Wilcox DA, Bubolz AH, Li R, Suzuki M, Zhang DX (2010) TRPV4-mediated endothelial Ca^{2+} influx and vasodilation in response to shear stress. Am J Physiol Heart Circ Physiol 298(2):H466–H476. doi:10.1152/ajpheart.00854.2009
20. Hartmannsgruber V, Heyken WT, Kacik M, Kaistha A, Grgic I, Harteneck C, Liedtke W, Hoyer J, Kohler R (2007) Arterial response to shear stress critically depends on endothelial TRPV4 expression. PLoS One 2(9):e827. doi:10.1371/journal.pone.0000827
21. Baratchi S, Tovar-Lopez FJ, Khoshmanesh K, Grace MS, Darby W, Almazi J, Mitchell A, McIntyre P (2014) Examination of the role of transient receptor potential vanilloid type 4 in endothelial responses to shear forces. Biomicrofluidics 8(4):044117. doi:10.1063/1.4893272
22. Misonou H, Mohapatra DP, Park EW, Leung V, Zhen DK, Misonou K, Anderson AE, Trimmer JS (2004) Regulation of ion channel localization and phosphorylation by neuronal activity. Nat Neurosci 7(7):711–718. doi:10.1038/nn1260
23. Magoski NS, Kaczmarek LK (1998) Direct and indirect regulation of a single ion channel. J Physiol Lond 509(1):1. doi:10.1111/j.1469-7793.1998.001bo.x
24. Wegierski T, Hill K, Schaefer M, Walz G (2006) The HECT ubiquitin ligase AIP4 regulates the cell surface expression of select TRP channels. EMBO J 25(24):5659–5669. doi:10.1038/sj.emboj.7601429
25. Xu H, Fu Y, Tian W, Cohen DM (2006) Glycosylation of the osmoresponsive transient receptor potential channel TRPV4 on Asn-651 influences membrane trafficking. Am J Physiol Renal Physiol 290(5):F1103–F1109. doi:10.1152/ajprenal.00245.2005
26. Arniges M, Fernandez-Fernandez JM, Albrecht N, Schaefer M, Valverde MA (2006) Human TRPV4 channel splice variants revealed a key role of ankyrin domains in multimerization and trafficking. J Biol Chem 281(3):1580–1586. doi:10.1074/jbc.M511456200
27. Lei L, Cao X, Yang F, Shi DJ, Tang YQ, Zheng J, Wang K (2013) A TRPV4 channel C-terminal folding recognition domain critical for trafficking and function. J Biol Chem 288(15):10427–10439. doi:10.1074/jbc.M113.457291
28. Cayouette S, Boulay G (2007) Intracellular trafficking of TRP channels. Cell Calcium 42(2):225–232. doi:10.1016/j.ceca.2007.01.014
29. Wegierski T, Lewandrowski U, Mueller B, Sickmann A, Walz G (2009) Tyrosine phosphorylation modulates the activity of TRPV4 in response to defined stimuli. J Biol Chem 284(5):2923–2933. doi:10.1074/jbc.M805357200
30. Poole DP, Amadesi S, Veldhuis NA, Abogadie FC, Lieu T, Darby W, Liedtke W, Lew MJ, McIntyre P, Bunnett NW (2013) Protease-activated receptor 2 (PAR(2)) Protein and transient receptor potential vanilloid 4 (TRPV4) protein coupling is required for sustained inflammatory signaling. J Biol Chem 288(8):5790–5802. doi:10.1074/jbc.M112.438184
31. Lu X, Gibbs JS, Hickman HD, David A, Dolan BP, Jin Y, Kranz DM, Bennink JR, Yewdell JW, Varma R (2012) Endogenous viral antigen processing generates peptide-specific MHC class I cell-surface clusters. Proc Natl Acad Sci USA 109(38):15407–15412. doi:10.1073/pnas.1208696109
32. Hoger JH, Ilyin VI, Forsyth S, Hoger A (2002) Shear stress regulates the endothelial Kir2.1 ion channel. Proc Natl Acad Sci USA 99(11):7780–7785. doi:10.1073/pnas.102184999
33. Barbier C, Boycott H, Eichel C, Louault F, Dilanian G, Coulombe A, Hatem S, Balse E (2014) Shear-stress triggered voltage-gated Kv1.5 channels exocytosis is altered in overloaded atria. Fundam Clin Pharmacol 28:79
34. Oancea E, Wolfe JT, Clapham DE (2006) Functional TRPM7 channels accumulate at the plasma membrane in response to fluid flow. Circ Res 98(2):245–253. doi:10.1161/01.RES.0000200179.29375.cc
35. Thorneloe KS, Cheung M, Bao W, Alsaid H, Lenhard S, Jian MY, Costell M, Maniscalco-Hauk K, Krawiec JA, Olzinski A, Gordon E, Lozinskaya I, Elefante L, Qin P, Matasic DS, James C, Tunstead J, Donovan B, Kallal L, Waszkiewicz A, Vaidya K, Davenport EA, Larkin J, Burgert M, Casillas LN, Marquis RW, Ye G, Eidam HS, Goodman KB, Toomey JR, Roethke TJ, Jucker BM, Schnackenberg CG, Townsley MI, Lepore JJ, Willette RN (2012) An orally active TRPV4 channel blocker prevents and resolves pulmonary edema induced by heart failure. Sci Trans Med 4(159):159ra148. doi:10.1126/scitranslmed.3004276
36. Sciaky N, Presley J, Smith C, Zaal KJ, Cole N, Moreira JE, Terasaki M, Siggia E, Lippincott-Schwartz J (1997) Golgi tubule traffic and the effects of brefeldin A visualized in living cells. J Cell Biol 139(5):1137–1155
37. Deborde S, Perret E, Gravotta D, Deora A, Salvarezza S, Schreiner R, Rodriguez-Boulan E (2008) Clathrin is a key regulator of basolateral polarity. Nature 452(7188):719–723. doi:10.1038/nature06828
38. Sandvig K, van Deurs B (2002) Transport of protein toxins into cells: pathways used by ricin, cholera toxin and Shiga toxin. FEBS Lett 529(1):49–53
39. De Matteis MA, Luini A (2008) Exiting the Golgi complex. Nat Rev Mol Cell Biol 9(4):273–284. doi:10.1038/nrm2378
40. Macia E, Ehrlich M, Massol R, Boucrot E, Brunner C, Kirchhausen T (2006) Dynasore, a cell-permeable inhibitor of dynamin. Dev Cell 10(6):839–850. doi:10.1016/j.devcel.2006.04.002
41. Lazaro-Dieguez F, Colonna C, Cortegano M, Calvo M, Martinez SE, Egea G (2007) Variable actin dynamics requirement for the exit of different cargo from the trans-Golgi network. FEBS Lett 581(20):3875–3881. doi:10.1016/j.febslet.2007.07.015
42. Becker D, Bereiter-Hahn J, Jendrach M (2009) Functional interaction of the cation channel transient receptor potential vanilloid 4 (TRPV4) and actin in volume regulation. Eur J Cell Biol 88(3):141–152. doi:10.1016/j.ejcb.2008.10.002
43. Fan HC, Zhang X, McNaughton PA (2009) Activation of the TRPV4 ion channel is enhanced by phosphorylation. J Biol Chem 284(41):27884–27891. doi:10.1074/jbc.M109.028803
44. Mamenko M, Zaika OL, Boukelmoune N, Berrout J, O'Neil RG, Pochynyuk O (2013) Discrete control of TRPV4 channel function in the distal nephron by protein kinases A and C. J Biol Chem 288(28):20306–20314. doi:10.1074/jbc.M113.466797
45. Lu HZ, Fedak PWM, Dai XJ, Du CQ, Zhou YQ, Henkelman M, Mongroo PS, Lau A, Yamabi H, Hinek A, Husain M, Hannigan G, Coles JG (2006) Integrin-linked kinase expression is elevated in human cardiac hypertrophy and induces hypertrophy in transgenic mice. Circulation 114(21):2271–2279. doi:10.1161/circulationaha.106.642330
46. Hannigan GE, LeungHagesteijn C, FitzGibbon L, Coppolino MG, Radeva G, Filmus J, Bell JC, Dedhar S (1996) Regulation of cell adhesion and anchorage-dependent growth by a new beta(1)-integrin-linked protein kinase. Nature 379(6560):91–96. doi:10.1038/379091a0
47. Lee SL, Hsu EC, Chou CC, Chuang HC, Bai LY, Kulp SK, Chen CS (2011) Identification and characterization of a novel integrin-

linked kinase inhibitor. J Med Chem 54(18):6364–6374. doi:10.1021/jm2007744
48. Tzima E, Irani-Tehrani M, Kiosses WB, Dejana E, Schultz DA, Engelhardt B, Cao G, DeLisser H, Schwartz MA (2005) A mechanosensory complex that mediates the endothelial cell response to fluid shear stress. Nature 437(7057):426–431. doi:10.1038/nature03952
49. Tzima E, del Pozo MA, Shattil SJ, Chien S, Schwartz MA (2001) Activation of integrins in endothelial cells by fluid shear stress mediates Rho-dependent cytoskeletal alignment. EMBO J 20(17):4639–4647. doi:10.1093/emboj/20.17.4639
50. Raftopoulou M, Hall A (2004) Cell migration: rho GTPases lead the way. Dev Biol 265(1):23–32. doi:10.1016/j.ydbio.2003.06.003
51. Baumer Y, Spindler V, Werthmann RC, Buenemann M, Waschke J (2009) Role of Rac 1 and cAMP in endothelial barrier stabilization and thrombin-induced barrier breakdown. J Cell Physiol 220(3):716–726. doi:10.1002/jcp.21819
52. Rebecca Soffe, Sara Baratchi, Shiyang Tang, Mahyar Nasabi, Peter McIntyre, Arnan Mitchell, Khashayar K (2015) Analysing calcium signalling of cells under high shear flows using discontinuous dielectrophoresis. Sci Rep. doi:10.1038/srep11973
53. Jaiswal JK, Rivera VM, Simon SM (2009) Exocytosis of post-Golgi vesicles is regulated by components of the endocytic machinery. Cell 137(7):1308–1319. doi:10.1016/j.cell.2009.04.064
54. Tomes CN (2015) The proteins of exocytosis: lessons from the sperm model. Biochem J 465(3):359–370. doi:10.1042/bj20141169
55. Chen JL, Ahluwalia JP, Stamnes M (2002) Selective effects of calcium chelators on anterograde and retrograde protein transport in the cell. J Biol Chem 277(38):35682–35687. doi:10.1074/jbc.M204157200
56. Porat A, Elazar Z (2000) Regulation of intra-Golgi membrane transport by calcium. J Biol Chem 275(38):29233–29237. doi:10.1074/jbc.M005316200
57. Hutcheson IR, Griffith TM (1997) Central role of intracellular calcium stores in acute flow- and agonist-evoked endothelial nitric oxide release. Br J Pharmacol 122(1):117–125. doi:10.1038/sj.bjp.0701340
58. Koo A, Nordsletten D, Umeton R, Yankama B, Ayyadurai S, Garcia-Cardena G, Dewey CF Jr (2013) In silico modeling of shear-stress-induced nitric oxide production in endothelial cells through systems biology. Biophys J 104(10):2295–2306. doi:10.1016/j.bpj.2013.03.052
59. Jones SM, Howell KE, Henley JR, Cao H, McNiven MA (1998) Role of dynamin in the formation of transport vesicles from the trans-Golgi network. Science 279(5350):573–577. doi:10.1126/science.279.5350.573
60. Liu X, Bandyopadhyay BC, Nakamoto T, Singh B, Liedtke W, Melvin JE, Ambudkar I (2006) A role for AQP5 in activation of TRPV4 by hypotonicity: concerted involvement of AQP5 and TRPV4 in regulation of cell volume recovery. J Biol Chem 281(22):15485–15495. doi:10.1074/jbc.M600549200
61. Becker D, Blase C, Bereiter-Hahn J, Jendrach M (2005) TRPV4 exhibits a functional role in cell-volume regulation. J Cell Sci 118(Pt 11):2435–2440. doi:10.1242/jcs.02372
62. Alenghat FJ, Nauli SM, Kolb R, Zhou J, Ingber DE (2004) Global cytoskeletal control of mechanotransduction in kidney epithelial cells. Exp Cell Res 301(1):23–30. doi:10.1016/j.yexcr.2004.08.003
63. Goswami C, Kuhn J, Heppenstall PA, Hucho T (2010) Importance of non-selective cation channel TRPV4 interaction with cytoskeleton and their reciprocal regulations in cultured cells. PLoS One 5(7):e11654. doi:10.1371/journal.pone.0011654
64. Ridley AJ (2001) Rho proteins: linking signaling with membrane trafficking. Traffic (Copenhagen, Denmark) 2(5):303–310
65. Symons M, Rusk N (2003) Control of vesicular trafficking by Rho GTPases. Curr Biol CB 13(10):R409–R418
66. Fiorio Pla A, Ong HL, Cheng KT, Brossa A, Bussolati B, Lockwich T, Paria B, Munaron L, Ambudkar IS (2012) TRPV4 mediates tumor-derived endothelial cell migration via arachidonic acid-activated actin remodeling. Oncogene 31(2):200–212. doi:10.1038/onc.2011.231
67. Kawasaki J, Davis GE, Davis MJ (2004) Regulation of Ca^{2+}-dependent K^+ current by alphavbeta3 integrin engagement in vascular endothelium. J Biol Chem 279(13):12959–12966. doi:10.1074/jbc.M313791200
68. Chao JT, Gui P, Zamponi GW, Davis GE, Davis MJ (2011) Spatial association of the Cav1.2 calcium channel with alpha5-beta1-integrin. Am J Physiol Cell Physiol 300(3):C477–C489. doi:10.1152/ajpcell.00171.2010
69. Carlson SS, Valdez G, Sanes JR (2010) Presynaptic calcium channels and alpha3-integrins are complexed with synaptic cleft laminins, cytoskeletal elements and active zone components. J Neurochem 115(3):654–666. doi:10.1111/j.1471-4159.2010.06965.x
70. Thodeti CK, Matthews B, Ravi A, Mammoto A, Ghosh K, Bracha AL, Ingber DE (2009) TRPV4 channels mediate cyclic strain-induced endothelial cell reorientation through integrin-to-integrin signaling. Circ Res 104(9):1123–1130. doi:10.1161/circresaha.108.192930
71. Ho B, Bendeck MP (2009) Integrin linked kinase (ILK) expression and function in vascular smooth muscle cells. Cell Adh Migr 3(2):174–176. doi:10.4161/cam.3.2.7374
72. Dedhar S, Williams B, Hannigan G (1999) Integrin-linked kinase (ILK): a regulator of integrin and growth-factor signalling. Trends Cell Biol 9(8):319–323
73. Tu YZ, Huang Y, Zhang YJ, Hua Y, Wu CY (2001) A new focal adhesion protein that interacts with integrin-linked kinase and regulates cell adhesion and spreading. J Cell Biol 153(3):585–598. doi:10.1083/jcb.153.3.585
74. Troussard AA, Mawji NM, Ong C, Mui A, St Arnaud R, Dedhar S (2003) Conditional knock-out of integrin-linked kinase demonstrates an essential role in protein kinase B/Akt activation. J Biol Chem 278(25):22374–22378. doi:10.1074/jbc.M303083200
75. Bellis A, Castaldo D, Trimarco V, Monti MG, Chivasso P, Sadoshima J, Trimarco B, Morisco C (2009) Cross-talk between PKA and Akt protects endothelial cells from apoptosis in the late ischemic preconditioning. Arterioscler Thromb Vasc Biol 29(8):1207–1212. doi:10.1161/atvbaha.109.184135
76. Hu Z, Xiong Y, Han X, Geng C, Jiang B, Huo Y, Luo J (2013) acute mechanical stretch promotes eNOS Activation in venous endothelial cells mainly via PKA and Akt pathways. PLoS One. doi:10.1371/journal.pone.0071359
77. Wu CY, Dedhar S (2001) Integrin-linked kinase (ILK) and its interactors: a new paradigm for the coupling of extracellular matrix to actin cytoskeleton and signaling complexes. J Cell Biol 155(4):505–510. doi:10.1083/jcb.200108077
78. Wierzbicka-Patynowski I, Niewiarowski S, Marcinkiewicz C, Calvete JJ, Marcinkiewicz MM, McLane MA (1999) Structural requirements of echistatin for the recognition of alpha(v)beta(3) and alpha(5)beta(1) integrins. J Biol Chem 274(53):37809–37814
79. Nilius B, Voets T (2013) The puzzle of TRPV4 channelopathies. EMBO Rep 14(2):152–163. doi:10.1038/embor.2012.219
80. O'Conor CJ, Leddy HA, Benefield HC, Liedtke WB, Guilak F (2014) TRPV4-mediated mechanotransduction regulates the metabolic response of chondrocytes to dynamic loading. Proc Natl Acad Sci USA 111(4):1316–1321. doi:10.1073/pnas.1319569111

81. Pochynyuk O, Zaika O, O'Neil RG, Mamenko M (2013) Novel insights into TRPV4 function in the kidney. Pflugers Arch 465(2):177–186. doi:10.1007/s00424-012-1190-z
82. Chen L, Kassmann M, Sendeski M, Tsvetkov D, Marko L, Michalick L, Riehle M, Liedtke WB, Kuebler WM, Harteneck C, Tepel M, Patzak A, Gollasch M (2015) Functional transient receptor potential vanilloid 1 and transient receptor potential vanilloid 4 channels along different segments of the renal vasculature. Acta Physiol 213(2):481–491. doi:10.1111/apha.12355
83. Sonkusare SK, Dalsgaard T, Bonev AD, Hill-Eubanks DC, Kotlikoff MI, Scott JD, Santana LF, Nelson MT (2014) AKAP150-dependent cooperative TRPV4 channel gating is central to endothelium-dependent vasodilation and is disrupted in hypertension. Sci Signal 7(333):14. doi:10.1126/scisignal.2005052
84. Sonkusare SK, Bonev AD, Ledoux J, Liedtke W, Kotlikoff MI, Heppner TJ, Hill-Eubanks DC, Nelson MT (2012) Elementary Ca2 + signals through endothelial TRPV4 channels regulate vascular function. Science 336(6081):597–601. doi:10.1126/science.1216283